

Proteomic profile of the lens in a streptozotocin-induced diabetic rat model using shotgun proteomics

NORIAKI NAGAI¹, TETSUSHI YAMAMOTO², KUNIKO MITAMURA² and ATSUSHI TAGA²

¹Department of Advanced Design for Pharmaceuticals; ²Pathological and Biomolecule Analyses Laboratory, Faculty of Pharmacy, Kindai University, Higashi-Osaka, Osaka 577-8502, Japan

Received June 30, 2017; Accepted September 14, 2017

DOI: 10.3892/br.2017.988

Abstract. Streptozotocin (STZ)-induced diabetic rats (STZ rats) were used to investigate diabetic cataracts. In the current study, a shotgun liquid chromatography (LC)/mass spectrometry (MS)-based global proteomic analysis method was used to examine the mechanism of lens opacification as a result of hyperglycemia in STZ rats. The 6-week old Wistar rats were injected with STZ for 2 days (100 mg/kg/day, i.p.) and housed for 3 weeks. The plasma glucose levels were identified to be significantly higher when compared with the normal rats and insulin was not detected in the STZ rats. Furthermore, opacification of the cortical epithelium was observed in the lenses of STZ rats. A total of 235 proteins were identified in the lenses of the STZ rats and 229 in the lenses of the normal rats. A label-free semi-quantitative method, based on spectral counting, identified 52 proteins that were differentially expressed in the lenses of STZ rats compared with normal rats. In particular, superoxide dismutase, which is a critical antioxidant enzyme that detoxifies superoxide through redox cycling, was downregulated when analyzed by the semi-quantitative method. In addition, phosphorylated-p38, which is important in the signaling pathway involved in the oxidative stress response, was significantly increased in the lenses of STZ rats when compared with normal rats ($P < 0.05$). Thus, the changes in protein expression were evaluated in the lenses of STZ rats using a shotgun LC/MS-based global proteomic analysis approach, and a decrease in antioxidant enzymes and an increase in oxidative stress were identified in the lenses of

STZ rats. Further studies are required to examine the role of these proteins in the onset or progression of diabetic cataracts.

Introduction

Diabetes mellitus is one of the most severe types of metabolic disorder in humans globally, and is characterized by insulin resistance and impaired insulin secretion (1). Long-term hyperglycemia in diabetics leads to many complications with tissues that require insulin for glucose entrance or with insulin-independent organs (2), and cataracts are one of the most common complications of exposure to uncontrolled chronic hyperglycemia in diabetes. It has been reported that the onset of cataracts in diabetic patients is 20 years earlier than in non-diabetic subjects (3).

Activation of the polyol pathway (4), non-enzymatic glycation of lens proteins (5-8) and increased oxidative stress (9-13) were reported as pathogenetic mechanisms of diabetic cataracts. In the polyol pathway, the excess glucose changes to sorbitol via aldose reductase and the excessive accumulation of sorbitol in the crystalline lens produces a high osmotic gradient, and causes the collapse and liquefaction of lens fibers, resulting in cataract formation (14,15). Furthermore, enhanced osmotic stress leads to the production of reactive oxygen species (ROS) in the crystalline lens (16-18). In addition, sorbitol is metabolized to fructose. The fructose is metabolized into fructose-3-phosphate and 3-deoxyglucosone (potent non-enzymatic glycation agents), which increase the quantity of advanced glycation end products leading to ROS generation (19,20). Thus, numerous studies have evaluated diabetic cataracts and model animals have been used.

Streptozotocin (STZ)-induced hyperglycemia in experimental animals (STZ rats) has been widely used as a valuable model to investigate the effect of different hypoglycemic agents (21). The STZ damages pancreatic β -cells in rats, leading to deficient insulin secretion and a diabetic model (22,23). The majority of diabetic rats are susceptible to the development of cataracts and lenticular polyol accumulation primarily induces cataractogenesis (14). However, all of the underlying mechanisms for lens opacification have not been elucidated in the STZ rats; therefore, further investigations are required. In the current study, a shotgun liquid chromatography (LC)/mass spectrometry (MS)-based global proteomic analysis of STZ rats was conducted to examine the underlying mechanism of

Correspondence to: Dr Atsushi Taga, Pathological and Biomolecule Analyses Laboratory, Faculty of Pharmacy, Kindai University, 3-4-1 Kowakae, Higashi-Osaka, Osaka 577-8502, Japan
E-mail: punk@phar.kindai.ac.jp

Abbreviations: LC/MS, liquid chromatography/mass spectroscopy; NSAF, normalized spectral abundance factor; ROS, reactive oxygen species; SOD, superoxide dismutase; STZ, streptozotocin

Key words: diabetic cataract, proteomics, lens, oxidative stress, streptozotocin-induced diabetic rats

lens opacification due to hyperglycemia. A total of 52 proteins were identified to be differentially expressed in the lenses of STZ rats compared with the lenses of normal rats, and these proteins may be involved in lens opacification.

Materials and methods

Materials. The following high-grade chemicals and reagents were purchased: Urea from GE Healthcare (Chicago, IL, USA) and thiourea from Nacalai Tesque, Inc. (Kyoto, Japan). All other chemicals and reagents were purchased from Wako Pure Chemical Industries, Ltd. (Osaka, Japan).

Animals. Healthy Male Wistar rats (mean weight, 220 g; n=10) were provided from the Kiwa Laboratory Animals Co., Ltd. (Wakayama, Japan) and the 6-week old rats were injected with STZ for 2 days (100 mg/kg/day via i.p. injection). As lens opacification was initially observed 2-3 weeks after STZ treatment, the rats were evaluated 3 weeks after the injection of STZ to elucidate the early mechanism of diabetic cataracts. All of the experiments were performed in compliance with the regulations approved by the Ethics Committee of the Kindai University Faculty of Pharmacy (Osaka, Japan). The rats were housed in a room at 25°C under a 12-h light/dark cycle (2-3 rats/cage). All rats had access to food and water *ad libitum*.

Assay of glucose and insulin. Blood (50 ml) was sampled without anesthesia from the tail vein of each rat after fasting for 12 h (10:00 a.m.). The plasma glucose level was measured using an Accutrend GCT (Roche Diagnostics GmbH, Mannheim, Germany), and plasma insulin levels were assayed using an ELISA Insulin kit (cat. no. M1103; Morinaga Institute of Biological Science, Inc., Kanagawa, Japan) according to the manufacturer's protocol (24). The dynamic range of the ELISA Insulin kit is 0.1-6.4 ng/ml.

Imaging of lens opacification in STZ rats. The rats were administered with 0.1% pivallephrine (Santen Pharmaceutical Co., Osaka, Japan) without anesthesia, and monitored using an EAS-1000 (Nidek Co., Ltd., Gamagori, Japan). The EAS-1000 conditions were as follows: Flash power index, 2,300±73; flash level, 100 W/sec; slit length and width, 5.0 mm.

Protein extraction from the lenses of STZ rats. Three weeks after injection, the STZ rats were euthanized, and the lenses of the STZ rats were removed and homogenized in urea lysis buffer (7 M urea, 2 M thiourea, 5% CHAPS and 1% Triton X-100). The protein concentration was measured using a Bio-Rad Protein Assay kit (Bio-Rad Laboratories, Inc., Hercules, CA, USA).

In-solution trypsin digestion. A gel-free digestion approach was performed in accordance with the protocol described by Bluemlein and Ralser (25). In brief, 10 µg protein extract from each sample was reduced by the addition of 45 mM dithiothreitol and 20 mM Tris(2-carboxyethyl)phosphine and alkylated using 100 mM iodoacetic acid. Following alkylation, samples were digested with trypsin gold, MS grade (Promega Corporation, Madison, WI, USA) at 37°C for 24 h. Subsequently, the digests were purified using PepClean C-18

Spin Columns (Thermo Fisher Scientific, Inc., Waltham, MA, USA) according to the manufacturer's protocol.

LC-MS/MS analysis for protein identification. Approximately 2 µg peptide samples were injected onto a peptide L-trap column (Chemicals Evaluation and Research Institute, Tokyo, Japan) using an HTC PAL Autosampler (CTC Analytics AG, Zwingen, Switzerland) and further separated through a Paradigm MS4 (AMR, Inc., Tokyo, Japan) using a reverse-phase C18-column (L-column, gel particle diameter, 3 µm; 120 Å; pore size, 0.2x150 mm; Chemicals Evaluation and Research Institute). The mobile phase consisted of solution A (0.1% formic acid in water) and solution B (acetonitrile). The column flow rate was 1 µl/min with a concentration gradient of acetonitrile, from 5% B to 40% B, for 120 min. Gradient-eluted peptides were analyzed using an LTQ ion-trap mass spectrometer (Thermo Fisher Scientific, Inc.). The results were acquired in a data-dependent manner in which MS/MS fragmentation was performed on the two most intense peaks of every full MS scan.

All MS/MS spectral data were searched against the SwissProt *Rattus Norvegicus* database using Mascot (version_2.4.01; Matrix Science, London, UK). The search criteria were set as follows: Enzyme, trypsin; allowance of up to two missed cleavage peptides; mass tolerance ± 2.0 Da and MS/MS tolerance ± 0.8 Da; and modifications of cysteine carbamidomethylation and methionine oxidation.

Semi-quantitative analysis of identified proteins. The fold changes in expressed proteins, on a base-2 logarithmic scale, were calculated using the R_{SC} , based on spectral counting (26). Relative quantities of identified proteins were also calculated using the normalized spectral abundance factor (NSAF) (27). Differentially expressed proteins were selected when their R_{SC} was >1 or <-1, which corresponded to fold changes of >2 or <0.5.

Western blot analysis. A total of 10 µg lens extract was added to each well and subjected to 10% SDS-PAGE under reducing conditions, and the separated proteins were transferred to polyvinylidene fluoride membranes for 30 min at 15 V. Following blocking in Tris-buffered saline Tween-20 (TBST) buffer (0.1%) with 5% skimmed milk for 2 h at room temperature, the membranes were incubated at 4°C overnight with anti-phosphorylated (p)-p38 mitogen-activated protein kinase (MAPK; 1;1,000; cat. no. 4511) and anti-p38 MAPK (cat. no. 8690) antibodies (both from Cell Signaling Technology, Inc., Danvers, MA, USA), along with anti-β-actin antibody (cat. no. sc-47778; Santa Cruz Biotechnology, Inc., Dallas, TX, USA) to confirm equal loading of the proteins. The membranes were washed three times with TBST and incubated with horseradish peroxidase-conjugated anti-rabbit immunoglobulin G antibody (cat. no. A106PU; American Qualex, San Clemente, CA, USA) for 1 h at room temperature. Following washing, the blots were visualized using SuperSignal West Dura Extended Duration substrate (Thermo Fisher Scientific, Inc.) and bands were detected using a myECL Imager system (version 2.0; Thermo Fisher Scientific, Inc.). Subsequently, the intensity of p-p38 and p38 were quantified using myImage Analysis software (version 2.0; Thermo Fisher

Scientific, Inc.) and the relative luminescence level of p-p38 over p38 was used to represent the signal strength of p-p38. All western blot analyses were performed in triplicate.

Statistical analysis. The unpaired Student's t-test was used and $P < 0.05$ was considered to indicate a statistically significant difference. All data are expressed as the standard error of the mean. The analyses were performed using GraphPad Prism software (version 5; GraphPad Software, Inc., La Jolla, CA, USA).

Results

Preparation of STZ-induced diabetic rats. Initially, the changes in plasma glucose and insulin were investigated in the rats following injection of STZ and whether the hyperglycemia caused lens opacification in the STZ rats was demonstrated. The plasma glucose levels in STZ rats (247.1 ± 10.6 mg/dl; $n=5$) were significantly higher than in the normal rats (81.3 ± 4.1 mg/dl; $n=5$). Furthermore, insulin was not detected in the STZ rats and the body weight in the STZ rats (217.3 ± 11.9 g; $n=5$) was significantly decreased when compared with that of the normal rats (319.5 ± 8.8 g; $n=5$). These results demonstrate that the STZ rats developed diabetes mellitus with hyperglycemia and hypoinsulinemia. In addition, opacification in the cortical epithelium was observed in the lenses of the STZ rats (Fig. 1).

Protein identification and profile of the lenses from STZ rats. To examine the effect of hyperglycemia on lens damage, the molecular profile of proteins whose expression level was changed in the diabetic rat model was investigated using shotgun proteomics. In the lenses of the STZ rats, 235 proteins were identified and 229 were identified in that of the normal rat (Normal) using the search parameters (Fig. 2). Among the 348 proteins identified in the rat lenses, 116 (33.3%) were identified in the two groups; while, 119 (34.2%) and 113 (32.5%) proteins were unique to STZ and normal rats, respectively (Fig. 2).

Subsequently, a label-free semi-quantitative method based on spectral counting was used to identify proteins with expression levels regulated by hyperglycemia. The R_{SC} value was plotted against the corresponding protein (x-axis) from left to right for proteins identified in the STZ and normal rats (Fig. 3). The positive and negative R_{SC} values indicate increased and decreased expression levels, respectively in the STZ rats. The NSAF value was plotted against the corresponding protein. The NSAF of proteins in the STZ and normal rats are indicated above and below the x-axis, respectively (Fig. 3). Proteins with either a high positive or negative R_{SC} value were considered to be candidate proteins, whose expression was likely regulated by hyperglycemia. A total of 52 differentially expressed proteins were identified in the lenses of the STZ rats (Table I). The expression levels of housekeeping proteins, such as β -actin and glyceraldehyde-3-phosphate dehydrogenase, did not change in the lenses of the normal and STZ rats (Fig. 3).

Effect of hyperglycemia on the p38 signaling pathway in the lenses of STZ rats. To determine whether the oxidative stress response by active oxygen is affected by downregulation of superoxide dismutase (SOD) expression, the phosphorylation

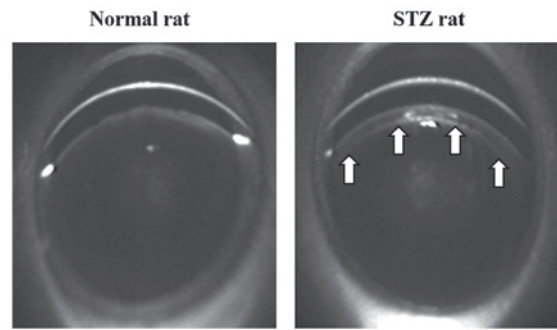


Figure 1. Scheimpflug slit images of lenses from normal rats and STZ-induced rats 3 weeks after injection of STZ. The images were obtained using an EAS-1000. Arrows indicate lens opacification. STZ, streptozotocin.

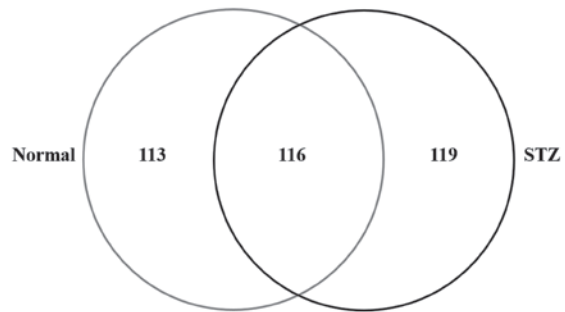


Figure 2. Venn map of proteins identified from the lenses of normal and STZ rats. There were 235 proteins identified in STZ-induced diabetic rats and 229 in the normal rats. STZ, streptozotocin.

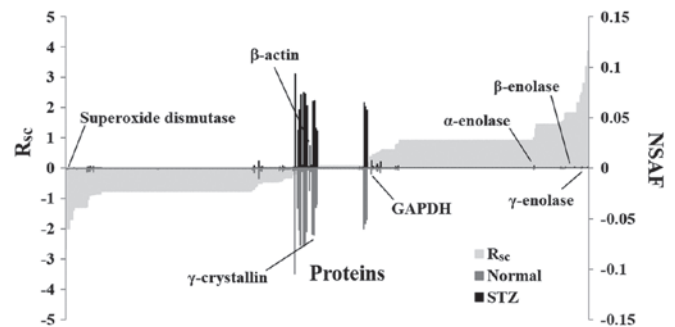


Figure 3. Semi-quantitative comparison of identified proteins in the lenses of STZ rats. The R_{SC} and NSAF values were calculated for the proteins identified (x-axis), and the protein expression was compared between the STZ-induced diabetic rats and the normal rats. Proteins highly expressed in either the STZ or the normal rats are presented near the right or left side of the x-axis. The housekeeping proteins are located around the center of the x-axis. STZ, streptozotocin; NSAF, normalized spectral abundance factor.

of p38, which is important in the signaling pathways involved in oxidative stress response, were examined. The phosphorylation of p38 in the lenses of STZ rats was significantly increased when compared with the lenses of normal rats ($P < 0.05$; Fig. 4).

Discussion

In the current study, a gel-free LC/MS-based proteomics approach was used to examine the effect of hyperglycemia on lens opacification. Although a quantitative value obtained using spectral counting may not be accurate (28), it is useful

Table I. Differentially expressed proteins in the lenses of STZ rats.

No.	ID	Accession number and description	Amino acids, n	Spectral counting		
				Normal	STZ	Fold change (R _{SC})
1	SODC_RAT	P07632: Superoxide dismutase [Cu-Zn]	154	4	0	-1.995
2	HDAC1_RAT	Q4QQW4: Histone deacetylase 1	482	4	0	-1.995
3	AK1CL_RAT	Q6AYQ2: Aldo-keto reductase family 1 member C21	318	3	0	-1.690
4	LGSN_RAT	Q7TT51: Lengsin	561	3	0	-1.690
5	ARRS_RAT	P15887: S-arrestin	403	5	1	-1.398
6	TERA_RAT	P46462: Transitional endoplasmic reticulum ATPase	806	2	0	-1.302
7	ATIF1_RAT	Q03344: ATPase inhibitor, mitochondrial	107	2	0	-1.302
8	RHOB_RAT	P62747: Rho-related GTP-binding protein RhoB	196	2	0	-1.302
9	ENTP6_RAT	Q9ER31: Ectonucleoside triphosphate diphosphohydrolase 6	455	2	0	-1.302
10	MYT1L_RAT	P70475: Myelin transcription factor 1-like protein	1,187	2	0	-1.302
11	RPGF2_RAT	F1M386: Rap guanine nucleotide exchange factor 2	1,496	2	0	-1.302
12	LMIP_RAT	P54825: Lens fiber membrane intrinsic protein	173	2	0	-1.302
13	HS71L_RAT	P55063: Heat shock 70 kDa protein 1-like	641	2	0	-1.302
14	ACTC_RAT	P68035: Actin, α cardiac muscle 1	377	30	11	-1.280
15	ACTG_RAT	P63259: Actin, cytoplasmic 2	375	25	11	-1.027
16	ENOA_RAT	P04764: α -enolase	434	11	22	1.006
17	KCRB_RAT	P07335: Creatine kinase B-type	381	1	4	1.301
18	K2C72_RAT	Q6IG04: Keratin, type II cytoskeletal 72	520	0	2	1.456
19	K1C14_RAT	Q6IFV1: Keratin, type I cytoskeletal 14	485	0	2	1.456
20	K1C13_RAT	Q6IFV4: Keratin, type I cytoskeletal 13	438	0	2	1.4563
21	PEBP1_RAT	P31044: Phosphatidylethanolamine-binding protein 1	187	0	2	1.456
22	COF1_RAT	P45592: Cofilin-1	166	0	2	1.456
23	NCAM1_RAT	P13596: Neural cell adhesion molecule 1	858	0	2	1.456
24	PGAM1_RAT	P25113: Phosphoglycerate mutase 1	254	0	2	1.456
25	PLEC_RAT	P30427: Plectin	4,687	0	2	1.456
26	NMDE1_RAT	Q00959: Glutamate receptor ionotropic, NMDA 2A	1,464	0	2	1.456
27	TCPG_RAT	Q6P502: T-complex protein 1 subunit γ	545	0	2	1.456
28	NPT2A_RAT	Q06496: Sodium-dependent phosphate transport protein 2A	637	0	2	1.456
29	KIFC1_RAT	Q5XI63: Kinesin-like protein KIFC1	693	0	2	1.456
30	RL18_RAT	P12001: 60S ribosomal protein L18	188	0	2	1.456
31	COPG1_RAT	Q4AEF8: Coatomer subunit γ -1	874	0	2	1.456
32	HSP7C_RAT	P63018: Heat shock cognate 71 kDa protein	646	0	2	1.456
33	PDE3B_RAT	Q63085: cGMP-inhibited 3~,5~-cyclic phosphodiesterase B	1,108	0	2	1.456
34	K2C75_RAT	Q6IG05: Keratin, type II cytoskeletal 75	542	4	13	1.521
35	K2C4_RAT	Q6IG00: Keratin, type II cytoskeletal 4	536	1	5	1.552
36	ENOB_RAT	P15429: β -enolase	434	2	8	1.588
37	TBA1C_RAT	Q6AYZ1: Tubulin α -1C chain	449	3	13	1.826
38	K2C8_RAT	Q10758: Keratin, type II cytoskeletal 8	483	0	3	1.844
39	K2C73_RAT	Q6IG03: Keratin, type II cytoskeletal 73	553	0	3	1.844
40	K2C7_RAT	Q6IG12: Keratin, type II cytoskeletal 7	457	0	3	1.844
41	ARF4_RAT	P61751: ADP-ribosylation factor 4	180	0	3	1.844
42	ARF1_RAT	P84079: ADP-ribosylation factor 1	181	0	3	1.844
43	TCAL7_RAT	D3ZT37: Transcription elongation factor A protein-like 7	98	0	3	1.844
44	TBB2B_RAT	Q3KRE8: Tubulin β -2B chain	445	0	3	1.844
45	K1C15_RAT	Q6IFV3: Keratin, type I cytoskeletal 15	447	0	4	2.149
46	K1C17_RAT	Q6IFU8: Keratin, type I cytoskeletal 17	433	0	4	2.149
47	K2C1B_RAT	Q6IG01: Keratin, type II cytoskeletal 1b	519	0	5	2.401
48	K2C5_RAT	Q6P6Q2: Keratin, type II cytoskeletal 5	576	2	16	2.490
49	ENOG_RAT	P07323: γ -enolase	434	0	7	2.802
50	K1C10_RAT	Q6IFW6: Keratin, type I cytoskeletal 10	526	0	7	2.802
51	K2C6A_RAT	Q4FZU2: Keratin, type II cytoskeletal 6A	552	0	11	3.374
52	K2C1_RAT	Q6IMF3: Keratin, type II cytoskeletal 1	625	0	16	3.869

Expression levels of these 52 proteins were >2-fold higher or lower in the lenses of STZ rats compared with in the lenses of normal rats. STZ, streptozotocin.

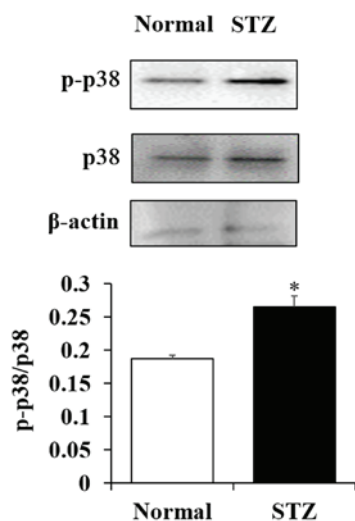


Figure 4. Effects of hyperglycemia on the p38 signaling pathway in the lens. The phosphorylation of p38 was significantly activated in the lenses of STZ-induced diabetic rats compared with in the lenses of normal rats. * $P < 0.05$. p-, phosphorylated; STZ, streptozotocin.

and has been used in previous studies investigating novel diagnostic biomarkers (29-34). Using semi-quantitative methods based on spectral counting, various proteins whose expression levels had changed by >2 -fold were successfully identified in the lenses of STZ rats. Representative proteins involved in enzyme-associated glycolysis, such as α -, β - and γ -enolase, were upregulated by the injection of STZ. These enhanced enzymes may be induced by high glucose. Although Quinlan *et al* (35) reported that keratin was not found in the adult human lens, certain keratin proteins (type II cytoskeletal 4, 5 and 75) were detected in the lenses of normal rats. Furthermore, the expression levels of those keratin proteins in the lenses of STZ rats were enhanced when compared with those of normal rats. The expression levels of keratin proteins in lenses may differ between humans and rats. Therefore, this requires further investigation in future studies.

Additionally, SOD, which is a critical antioxidant enzyme that detoxifies superoxides via redox cycling and histone deacetylase 1 were downregulated. It is well known that chronic hyperglycemia increases the oxidant load (11) and leads to the onset of cataracts (12). Furthermore, the antioxidant capacity is reduced and the free radical load is increased in the eyes of diabetes mellitus patients. This change increases the susceptibility of the crystalline lens to oxidative damage (13). In addition, decrease in the antioxidant capacity is facilitated by advanced glycation and defects in antioxidant enzyme activity (13). Maurya *et al* (36) identified that the serum of SOD was significantly lower in patients with diabetic cataracts (9.13 U/ml) compared with patients with senile cataracts (25.30 U/ml) (36). These findings indicate that activation of the p38 signaling pathway, via downregulation of SOD expression, is one of the factors involved in the onset of lens opacification and that dysfunction of transcription, via low histone deacetylase 1, may be associated with the development of diabetic cataracts in STZ rats. Further studies are required to validate the results of spectral counting by western blotting and to elucidate the precise mechanisms for p38 in hyperglycemia-associated lens opacification using

p38 inhibitors or corresponding knockout/knock-in strategies. In addition, it is important to validate these findings in human tissues. Therefore, our future studies will investigate the expression levels of SOD and p38 in human lens epithelial (HLE) SRA 01/04 cells exposed to high glucose conditions.

In conclusion, the changes in protein expression levels in the lenses of STZ rats were evaluated using a shotgun LC/MS-based global proteomic analysis, and an increase in oxidative stress in the lenses of STZ rats was observed. Therefore, oxidative stress may serve important roles in the progression of diabetic cataracts.

Acknowledgements

The present study was supported in part by a Grant-in-Aid for Scientific Research from the Japan Society for the Promotion of Science to T. Yamamoto (grant no. 15K09054).

References

- Expert Committee on the Diagnosis and Classification of Diabetes Mellitus: Report of the expert committee on the diagnosis and classification of diabetes mellitus. *Diabetes Care* 26 (Suppl 1): S5-S20, 2003.
- Brownlee M: Biochemistry and molecular cell biology of diabetic complications. *Nature* 414: 813-820, 2001.
- Hashim Z and Zarina S: Osmotic stress induced oxidative damage: Possible mechanism of cataract formation in diabetes. *J Diabetes Complications* 26: 275-279, 2012.
- Srivastava SK, Ramana KV and Bhatnagar A: Role of aldose reductase and oxidative damage in diabetes and the consequent potential for therapeutic options. *Endocr Rev* 26: 380-392, 2005.
- Ahmed N: Advanced glycation endproducts - role in pathology of diabetic complications. *Diabetes Res Clin Pract* 67: 3-21, 2005.
- Araki N, Ueno N, Chakrabarti B, Morino Y and Horiuchi S: Immunochemical evidence for the presence of advanced glycation end products in human lens proteins and its positive correlation with aging. *J Biol Chem* 267: 10211-10214, 1992.
- Duhaiman AS: Glycation of human lens proteins from diabetic and (nondiabetic) senile cataract patients. *Glycoconj J* 12: 618-621, 1995.
- Lyons TJ, Silvestri G, Dunn JA, Dyer DG and Baynes JW: Role of glycation in modification of lens crystallins in diabetic and nondiabetic senile cataracts. *Diabetes* 40: 1010-1015, 1991.
- Nagaraj RH, Sell DR, Prabhakaram M, Ortwerth BJ and Monnier VM: High correlation between pentosidine protein crosslinks and pigmentation implicates ascorbate oxidation in human lens senescence and cataractogenesis. *Proc Natl Acad Sci USA* 88: 10257-10261, 1991.
- Shamsi FA, Sharkey E, Creighton D and Nagaraj RH: Maillard reactions in lens proteins: Methylglyoxal-mediated modifications in the rat lens. *Exp Eye Res* 70: 369-380, 2000.
- Agte VV and Tarwadi KV: Combination of diabetes and cataract worsens the oxidative stress and micronutrient status in Indians. *Nutrition* 24: 617-624, 2008.
- Jeganathan VS, Wang JJ and Wong TY: Ocular associations of diabetes other than diabetic retinopathy. *Diabetes Care* 31: 1905-1912, 2008.
- Ookawara T, Kawamura N, Kitagawa Y and Taniguchi N: Site-specific and random fragmentation of Cu,Zn-superoxide dismutase by glycation reaction. Implication of reactive oxygen species. *J Biol Chem* 267: 18505-18510, 1992.
- Kinoshita JH: Mechanisms initiating cataract formation. *Proctor Lecture. Invest Ophthalmol* 13: 713-724, 1974.
- Kinoshita JH: Cataracts in galactosemia. The Jonas S. Friedenwald Memorial Lecture. *Invest Ophthalmol* 4: 786-799, 1965.
- Pollreisz A and Schmidt-Erfurth U: Diabetic cataract-pathogenesis, epidemiology and treatment. *J Ophthalmol* 2010: 608751, 2010.
- Takamura Y, Sugimoto Y, Kubo E, Takahashi Y and Akagi Y: Immunohistochemical study of apoptosis of lens epithelial cells in human and diabetic rat cataracts. *Jpn J Ophthalmol* 45: 559-563, 2001.

18. Li WC, Kuszak JR, Dunn K, Wang RR, Ma W, Wang GM, Spector A, Leib M, Cotliar AM, Weiss M, *et al*: Lens epithelial cell apoptosis appears to be a common cellular basis for non-congenital cataract development in humans and animals. *J Cell Biol* 130: 169-181, 1995.
19. Tang WH, Martin KA and Hwa J: Aldose reductase, oxidative stress, and diabetic mellitus. *Front Pharmacol* 3: 87, 2012.
20. Stitt AW: The maillard reaction in eye diseases. *Ann N Y Acad Sci* 1043: 582-597, 2005.
21. Ivorra MD, Payá M and Villar A: A review of natural products and plants as potential antidiabetic drugs. *J Ethnopharmacol* 27: 243-275, 1989.
22. Stephen Irudayaraj S, Sunil C, Duraipandiyan V and Ignacimuthu S: Antidiabetic and antioxidant activities of *Toddalia asiatica* (L.) Lam. leaves in streptozotocin induced diabetic rats. *J Ethnopharmacol* 143: 515-523, 2012.
23. Nisha P and Mini S: Flavanoid rich ethyl acetate fraction of *Musa paradisiaca* inflorescence down-regulates the streptozotocin induced oxidative stress, hyperglycaemia and mRNA levels of selected inflammatory genes in rats. *J Funct Foods* 5: 1838-1847, 2013.
24. Nagai N, Ito Y and Sasaki H: Hyperglycemia enhances the production of amyloid β 1-42 in the lenses of Otsuka Long-Evans Tokushima fatty rats, a model of human type 2 diabetes. *Invest Ophthalmol Vis Sci* 57: 1408-1417, 2016.
25. Bluemlein K and Ralser M: Monitoring protein expression in whole-cell extracts by targeted label- and standard-free LC-MS/MS. *Nat Protoc* 6: 859-869, 2011.
26. Old WM, Meyer-Arendt K, Aveline-Wolf L, Pierce KG, Mendoza A, Sevinsky JR, Resing KA and Ahn NG: Comparison of label-free methods for quantifying human proteins by shotgun proteomics. *Mol Cell Proteomics* 4: 1487-1502, 2005.
27. Zybailov B, Coleman MK, Florens L and Washburn MP: Correlation of relative abundance ratios derived from peptide ion chromatograms and spectrum counting for quantitative proteomic analysis using stable isotope labeling. *Anal Chem* 77: 6218-6224, 2005.
28. Lundgren DH, Hwang SI, Wu L and Han DK: Role of spectral counting in quantitative proteomics. *Expert Rev Proteomics* 7: 39-53, 2010.
29. Yamamoto T, Kudo M, Peng WX and Naito Z: Analysis of protein expression regulated by lumican in PANC 1 cells using shotgun proteomics. *Oncol Rep* 30: 1609-1621, 2013.
30. Takaya A, Peng WX, Ishino K, Kudo M, Yamamoto T, Wada R, Takeshita T and Naito Z: Cystatin B as a potential diagnostic biomarker in ovarian clear cell carcinoma. *Int J Oncol* 46: 1573-1581, 2015.
31. Kanzaki A, Kudo M, Ansai S, Peng WX, Ishino K, Yamamoto T, Wada R, Fujii T, Teduka K, Kawahara K, *et al*: Insulin-like growth factor 2 mRNA-binding protein-3 as a marker for distinguishing between cutaneous squamous cell carcinoma and keratoacanthoma. *Int J Oncol* 48: 1007-1015, 2016.
32. Yamamoto T, Kudo M, Peng WX, Takata H, Takakura H, Teduka K, Fujii T, Mitamura K, Taga A, Uchida E and Naito Z: Identification of aldolase A as a potential diagnostic biomarker for colorectal cancer based on proteomic analysis using formalin-fixed paraffin-embedded tissue. *Tumour Biol* 37: 13595-13606, 2016.
33. Takata H, Kudo M, Yamamoto T, Ueda J, Ishino K, Peng WX, Wada R, Tani N, Yoshida H, Uchida E and Naito Z: Increased expression of PDIA3 and its association with cancer cell proliferation and poor prognosis in hepatocellular carcinoma. *Oncol Lett* 12: 4896-4904, 2016.
34. Kawamura T, Nomura M, Tojo H, Fujii K, Hamasaki H, Mikami S, Bando Y, Kato H and Nishimura T: Proteomic analysis of laser-microdissected paraffin-embedded tissues: (I) Stage-related protein candidates upon non-metastatic lung adenocarcinoma. *J Proteomics* 73: 1089-1099, 2010.
35. Quinlan RA, Sandilands A, Procter JE, Prescott AR, Hutcheson AM, Dahm R, Gribbon C, Wallace P and Carter JM: The eye lens cytoskeleton. *Eye (Lond)* 13 (Pt 3b): 409-416, 1999.
36. Maurya OP, Mohanty L, Bhaduri G and Chandra A: Role of anti-oxidant enzymes superoxide dismutase and catalase in the development of cataract: Study of serum levels in patients with senile and diabetic cataracts. *J Indian Med Assoc* 104: 394, 396-397, 2006.